# Fucoxanthin-rich fraction from *Sargassum fusiformis* alleviates particulate matter-induced inflammation *in vitro* and *in vivo*

Yu-Lin Dai [a,b,c], Yun-Fei Jiang [b], Yu-An Lu [b], Jiang-Bo Yu [c], Min-Cheol Kang [d,*], You-Jin Jeon [b,e,*]

[a] *Jilin Ginseng Academy, Changchun University of Chinese Medicine, Changchun 130117, China*
[b] *Department of Marine Life Science, Jeju National University, Jeju 63243, Republic of Korea*
[c] *Postdoctoral Work Station of Jilin Aodong Medicine Group Co., Ltd., Dunhua 133700, China*
[d] *Research Group of Food Processing, Research Division of Strategic Food Technology, Korea Food Research Institute (KFRI), Wanju 55365, Republic of Korea*
[e] *Marine Science Institute, Jeju National University, Jeju 63333, Republic of Korea*

## ARTICLE INFO

## ABSTRACT

Particulate matter (PM) contributes to air pollution and primarily originates from unregulated industrial emissions and seasonal natural dust emissions. Fucoxanthin (Fx) is a marine natural pigment from brown macroalgae that has been shown to have various beneficial effects on health. However, the effects of Fx on PM-induced toxicities in cells and animals have not been assessed. In this study, we investigated the anti-inflammatory potential of the Fx-rich fraction (FxRF) of *Sargassum fusiformis* against PM-mediated inflammatory responses. The FxRF composition was analyzed by rapid-resolution liquid chromatography mass spectrometry. Fx and other main pigments were identified. FxRF attenuated the production of inflammatory components, including prostaglandin E2 ($PGE_2$), cyclooxygenase-2, interleukin (IL)-1$\beta$, and IL-6 from PM-exposed HaCaT keratinocytes. PM exposure also reduced the levels of nitric oxide (NO), tumor necrosis factor-$\alpha$, inducible nitric oxide synthase (iNOS), and $PGE_2$ in PM-exposed RAW264.7 macrophages. Additionally, the culture medium from PM-exposed HaCaT cells induced upregulation of NO, iNOS, $PGE_2$, and pro-inflammatory cytokines in RAW264.7 macrophages. FxRF also significantly decreased the expression levels of factors involved in inflammatory responses, such as NO, reactive oxygen species, and cell death, in PM-exposed zebrafish embryos. These results demonstrated the potential protective effects of FxRF against PM-induced inflammation both *in vitro* and in a zebrafish model.

## 1. Introduction

Particulate matter (PM) is the main contributor to air contamination. PM primarily originates from unregulated industrial emissions and seasonal natural dust emissions [1,2]. In modern China, increases in coal-burning thermal power plants, petrol and diesel consumption by vehicles, and agricultural activities have contributed to the occurrence of haze or smog episodes [3,4]. PM often contains potentially toxic metals in the form of aerosols at concentrations higher than natural concentrations [5,6]. PM particles pose a high risk to health; they can lead to the development of lung cancer, chronic respiratory and heart diseases, and immune system dysfunction [7]. These particles are believed to be pathogenic and adversely affect the human body by causing respiratory complications and inducing inflammatory and allergic reactions [8,9]. Previous research has described the potential toxicological mechanisms [10] and gene expression [11] that link PM and its effects on human epidermal keratinocytes.

Fucoxanthin (Fx), a marine natural pigment, is a carotenoid abundantly present in brown macroalgae, such as *Phaeodactylum tricornutum*, *Laminaria japonica*, *Eisenia bicyclis*, *Undaria pinnatifida*, and *Sargassum*
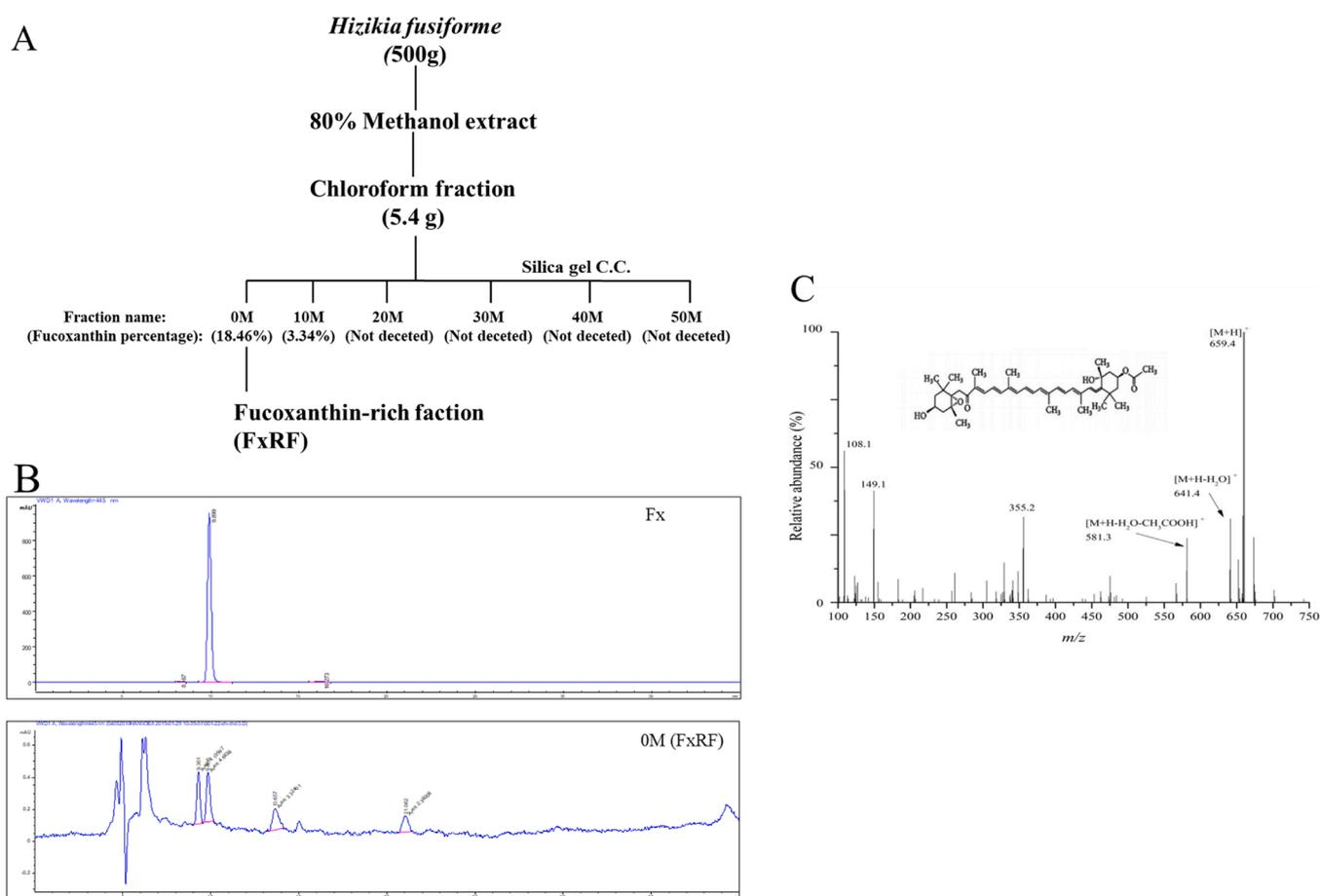
**Fig. 1.** Chemical information of fucoxanthin-rich fraction (FxRF) from *Sargassum fusiformis*. (A) Extraction and isolation scheme for FxRF. (B) The HPLC chromatographs of Fx standard and FxRF. The mobile phases used in the isocratic elution consisted of eluent: 0.1% formic acid water and 95% methanol. The flow rate was 0.3 mL/min and UV detection was observed at 445 nm. (C) The mass spectrum of fucoxanthin from FxRF.

*siliquastrum* [12–14]. These seaweeds serve as traditional foods in Asian countries. Fx exerts antioxidant, anticancer, anti-inflammatory, and anti-ultraviolet (UV) effects [13,15–17]. Because seaweeds contain relatively low Fx contents (0.02–0.58% fresh weight), obtaining sufficient quantities of Fx for commercial application is a major challenge [18]. However, extracts of the fucoxanthin-rich fraction (FxRF), which contain Fx and other similar bioactive pigments, are easy to obtain.

*Sargassum fusiformis* is a well-known type of brown seaweed in Eastern Asia and has been used as a folk medicinal ingredient for thousands of years. In a recent study, *S. fusiformis* was found to have high concentrations of heavy metals, such as arsenic, which induces a series of metabolic disorders in humans. In our previous studies, we found that the heavy metal content could be significantly decreased using acid-hot water processing [19,20]. An FxRF from *Hizikia fusiforme* showed higher DPPH radical scavenging activity than those from *Undaria pinnatifida* and *S. fulvellum* [21]. However, little information is available regarding the anti-inflammatory activities of FxRF from *S. fusiformis* on PM-induced inflammation.

Therefore, in this study, we assessed the anti-inflammatory activities of FxRF from *S. fusiformis* against PM-induced inflammation *in vitro* and *in vivo*.

## 2. Materials and methods

### 2.1. Preparation of FxRF

*S. fusiformis* was purchased from a commercial dealer in Dongtou, Zhejiang province, China, in May 2018. The length of fresh seaweed

*S. fusiformis* is ranged from 20−60 cm. The sample was cleaned by tap water to remove debris. Heavy metal of the sample was decreased by acid-hot water processing followed our previous method [19]. The *S. fusiformis* (500 g) powder was shaken with 80% methanol for 24 h. The extract was then partitioned with water and chloroform. The chloroform layer (5.4 g) was separated by silica column chromatography; the mobile phase was selected as a chloroform-methanol mixture (100:0, 90:10, 80:20, 70:30, 60:40, and 50:50) to obtain separated fractions; the active fractions were marked as 0 M (M is short for the ratio of methanol), 10 M, 20 M, 30 M, 40 M, and 50 M, respectively. According to chemical analysis, 0 M showed the highest relative Fx content; therefore, we used this fraction as FxRF (Fig. 1A).

### 2.2. Chemical analysis of FxRF

High-performance liquid chromatography (HPLC; Agilent 1220 Infinity LC system; Agilent Technologies Inc., Santa Clara, CA, USA) was carried out to quantify the compounds [22]. The structure of the main compound was compared with a commercial Fx standard (cat. no. 16337; Sigma-Aldrich, St. Louis, MO, USA) based on a previous report [23]. A 10-μL sample was injected into the Agilent 1220 Infinity LC system. The column was used in a Proshell 120 EC-$C_{18}$ (150 mm × 4.6 mm, 4 μm; Agilent Technologies Inc.). The mobile phases used in the isocratic elution consisted of eluent (A) comprising 0.1% formic acid distilled water and eluent (B) comprising 95% methanol. The flow rate was 0.3 mL/min, and UV detection was observed at 445 nm. The Fx was eluted at a retention time of 9.899 min (Fig. 1B). The Fx standard was used to calibrate the standard curve and retention times with six

continuously increasing concentrations. Agilent ChemStation software (Waldbronn, Germany) was used to acquire peak areas.

A liquid chromatography system (Agilent 1200 RRLC; Agilent Technologies Inc.) coupled with a mass spectrometer (Agilent 6520 Q-TOF-MS; Agilent Technologies Inc.) in positive ion mode was used for analysis. An Agilent Eclipse Plus $C_{18}$ column (2.1 mm × 150 mm, 3.5 μm) at 30 °C was used to separate samples. The flow rate was 0.3 mL/min, and the injected volume was set to 5 μL. The mobile phases and isocratic elution mode followed that of HPLC analysis. The parameters for mass spectrometry were set as follows: atomization gas pressure of $2.41 \times 10^5$ Pa, nebulizer of 30 psig, cone voltage of 35 V, capillary voltage of 2800 V, fragmentation voltage of 120 V, drying gas flow rate of 0.8 mL/min, drying gas temperature of 350 °C, and mass range of *m/z* 100–2000.

### 2.3. Cell culture

RAW264.7 macrophages and HaCaT keratinocytes were obtained from the Korean Cell Line Bank (KCLB, Seoul, Korea). Dulbecco's modified Eagle's medium containing 10% fetal bovine serum and 1% penicillin/streptomycin (Thermo Fisher Scientific, Waltham, MA, USA) was used to cultured cells.

### 2.4. Nuclear staining and reactive oxygen species (ROS) measurement

The protective properties of FxRF against PM-stimulated apoptosis in keratinocytes were observed following analysis of Hoechst 33342/propidium iodide (PI) nuclear staining and 2,7-dichlorofluorescein diacetate (DCFH-DA) assay. Keratinocytes were seeded at a density of $1 \times 10^5$ cells/mL in 24-well culture wells, and after 24 h incubation, various concentrations of FxRF were added. The cells were then treated with 125 μg/mL PM. PM was collected from Beijing, China, and morphological and compositional analyses of PM were performed in our previous study; the dose of PM (125 μg/mL) *in vitro* was followed in the previous study as well [24]. Fresh medium was added after incubation for 30 min. Next, a 25-μL volume of Hoechst 33342 (stock 1 mg/mL)/PI (5 μg/mL) nuclear staining solution and a 25-μL volume of DCFH-DA solution (25 μM) were added to cells for 24 h incubation. Cells were imaged using a fluorescence microscope coupled with a CoolSNAP-Pro color digital camera (Meyer Instruments, Inc., Houston, TX, USA) after 10 min of staining in the dark [25].

### 2.5. Evaluation of inflammatory responses

Macrophages and keratinocytes were seeded separately in different 24-well plates. After incubation for 24 h, the indicated concentrations of FxRF were added to the cells, and cells were incubated for an additional 1 h. Then, PM (125 μg/mL) was added to the indicated wells. Fresh medium was added and an additional 30-min incubation, and cells were continuously incubated for another 24 h. The culture medium was collected to measure the levels of inflammation-related mediators and cytokines. The cells were stained in 3 h with 2 mg/mL of MTT solution in the dark for cell viability measurement and stained in 10 min with 5 μg/mL of DCFH-DA solution in the dark for ROS level detection. In keratinocytes, cell viability, intracellular ROS, inflammation-related mediators, and cytokines were investigated by 3-(4,5-dimethylthiazol-2-yl)-2,5-diphenyltetrazolium bromide (MTT) assays, DCFH-DA assays, and commercial kits (R&D Systems Inc., Minneapolis, MN, USA) [26]. Heavy metals influence the value of MTT assays because the assays are colorimetric assays. Therefore, to avoid the influence of heavy metals on cell viability, the dimethyl sulfoxide solution containing formazan was centrifuged (8000 × *g* for 5 min), and the supernatant was measured at 540 nm. The cell medium was harvested to measure the expression of inflammatory-related mediators and cytokines using commercial enzyme-linked immunosorbent assay kits. The analysis was performed according to the manufacturer's guidelines. In macrophages, the PM

concentration, cell viability, nitric oxide (NO) production, and inflammation-related mediators and cytokines were evaluated according to previous protocols [24].

The seeded keratinocytes were exposed to the indicated concentrations of FxRF, and inflammation was induced by PM for 30 min. The cells were replaced with fresh medium and continuously incubated for 24 h. Then, the culture medium of PM-induced keratinocytes (H-PM) was treated with the preseeded macrophages in real time, and inflammation-related mediators and cytokines were evaluated.

### 2.6. Western blot analysis

Keratinocytes and macrophages were harvested after FxRF and PM or H-PM treatment, and cells were then homogenized with lysis buffer. The supernatants of the lysates were obtained by centrifugation, and protein content was measured using a commercial kit. Lysis buffer containing 30 μg protein was separated on a polyacrylamide gel (12%). The proteins were then transferred onto nitrocellulose membranes. A solution containing 5% nonfat milk was used to block the membranes for 3 h, and the membranes were then incubated with primary antibodies (β-actin, p38 MAPK, P-p38 MAPK, Erk1/2, P-Erk1/2, JNK, P-JNK, iNOS, and COX-2 (Santa Cruz Biotechnology) (4 °C for 8 h), followed by incubation with secondary antibodies (anti-mouse IgG, Santa Cruz Biotechnology) at room temperature for 3 h. A chemiluminescent substrate was employed to develop the blots. The fluorescence images and calculation of band intensity were performed as previously reported [27].

### 2.7. Zebrafish embryo experiments

Zebrafish were obtained and cultured with a light/dark cycle at room temperature. According to a previous protocol [24], a PM concentration of 10 μg/mL was selected for each well. PM-induced NO, ROS production, and cell death in embryos were evaluated. Briefly, the embryos were randomly transferred to 12-well plates and treated with different concentrations of FxRF followed by PM treatment. After incubation for 72 h, 4-amino-5-methylamino-2′,7′-difluorofluorescein diacetate, DCFH-DA, and acridine orange were used as fluorescent dyes to identify NO production, ROS levels, and cell death of hatched larvae, respectively. The fluorescence intensity of embryos was determined using a spectrofluorometer (Perkin-Elmer LS-5B, Austria). All animal assays were approved by the Animal Care and Use Committee of Jeju National University.

### 2.8. Statistical analysis

The assays in this study were carried out in three independent experiments. Values are expressed as means ± standard errors (SEs). One-way analysis of variance was used to analyze the mean values in GraphPad Prism 5. Student's t-tests were employed to calculate significant differences between means. Results with *p* value of less than 0.05 were considered significant.

## 3. Results

### 3.1. HPLC and rapid-resolution liquid chromatography mass spectrometry (RRLC-MS) analysis of FxRF

HPLC analysis of six active fractions (0 M, 10 M, 20 M, 30 M, 40 M, and 50 M) from *S. fusiformis* was conducted. As shown in Fig. 1B, based on the peak areas, 0 M contained the highest concentration of Fx (18.46%) among the six fractions tested. Subsequently, RRLC-MS was carried out for identification of Fx. The $[M+H]^+$ ion (*m/z* 659.3) and the adduct $[M + Na]^+$ ion (*m/z* 681.9) were identified based on the fragment pattern shown in Fig. 1C. The daughter ions of Fx at *m/z* 581.4 and 641.4 were generated by loss of $H_2O$ and $H_2O + CH_3COOH$,
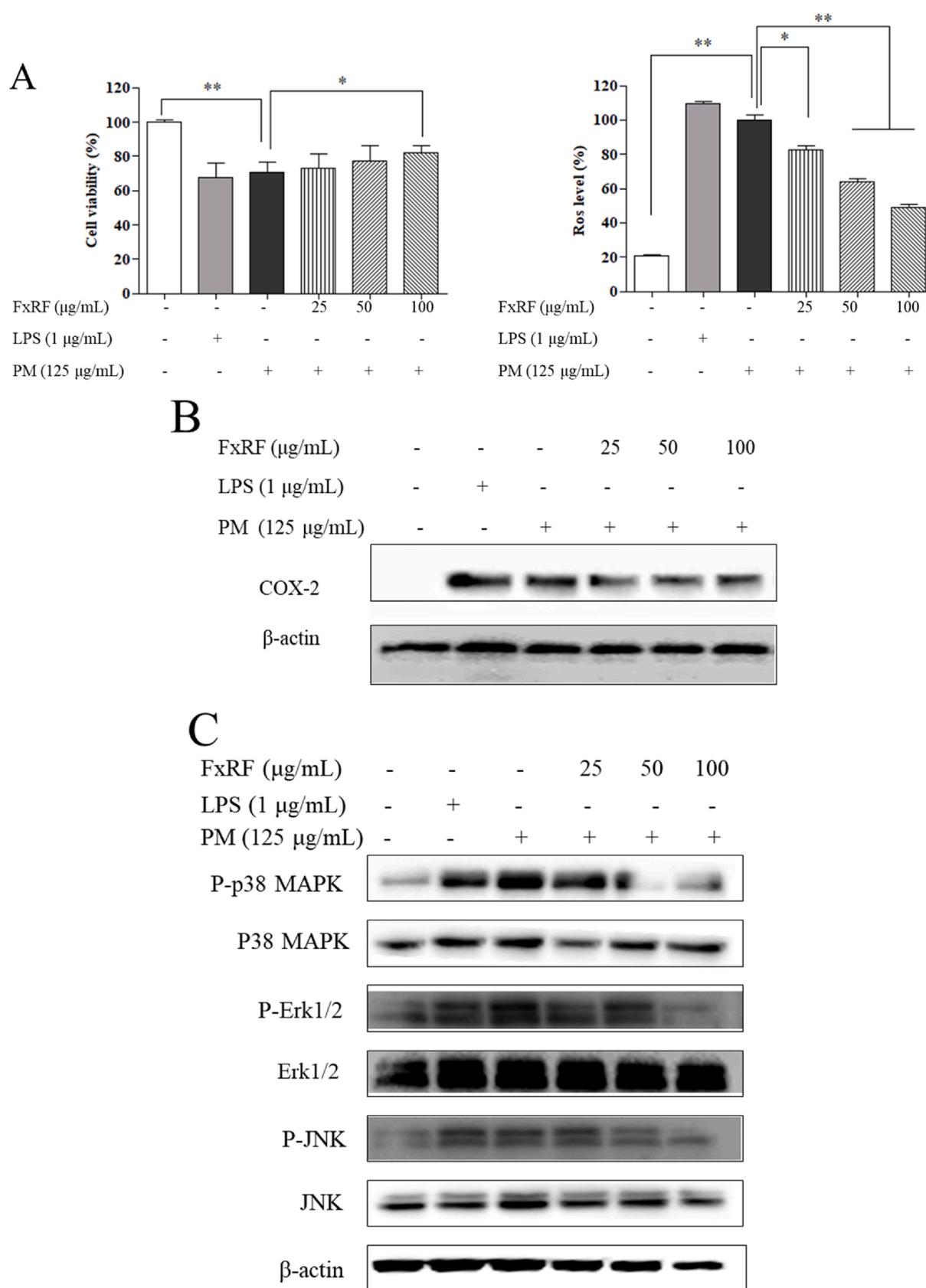
**Fig. 2.** Efficacy of FxRF against inflammation induced by PM in HaCaT keratinocytes (A), and analyses of HaCaT cell viability and intracellular ROS levels; (B) Western blot analyses of COX-2 expressions; (C) levels of key molecular mediators in the MAPK pathways; and (D) ELISA of PGE$_2$ and pro-inflammatory cytokines (IL-1β, IL-6, and TNF-α). Pre-seeded cells ($1 \times 10^5$ cells/mL) were treated with different FxRF concentrations after 24 h and stimulated with PM after 30 min. Cells were harvested after 24 h to measure inflammatory mediators (COX-2 and PGE$_2$) and pro-inflammatory cytokines (IL-1β, IL-6, and TNF-α). Apoptotic body formation was observed under a fluorescence microscope after (E) DCFH-DA treatment and (F) Hoechst 33,342 and PI staining. Graphical representations are means ± standard error (SE) based on three replications. *$p < 0.05$ and **$p < 0.01$ indicate that the values were significantly different from those for the PM-treated group..
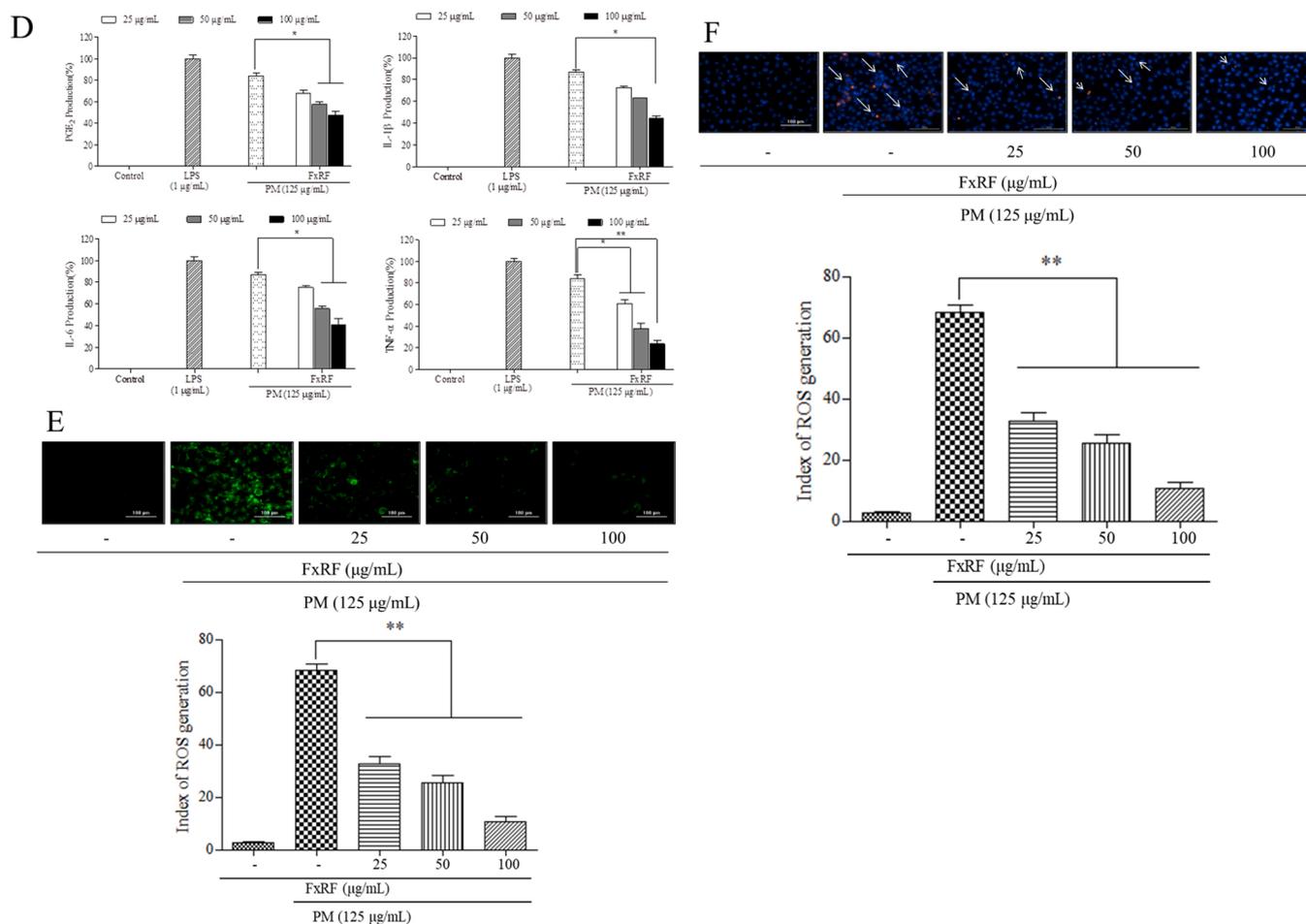
**Fig. 2.** (*continued*).

respectively. Thus, the characteristic ion $m/z$ 581.4 and 641.4 peaks in the mass spectrum matched that of Fx. In addition, other compounds, mainly pigments, such as pheophytin-a, chlorophyll-a, and β-carotene, were identified by determination of molecular weight and fragments. The identified compounds were in good agreement with published articles [28,29].

### 3.2. Effects of FxRF on PM-induced inflammatory responses in keratinocytes

The production of inflammatory mediators and cytokines in PM-induced keratinocytes was evaluated by MTT and DCFH-DA assays. The lipopolysaccharide (LPS)-treated group was regarded as a positive control. We found that LPS treatment increased ROS levels and decreased the viability of HaCaT keratinocytes. The cytoprotective effects of FxRF on PM-exposed HaCaT keratinocytes (Fig. 2A) were also observed. In cell viability assays, we found high SE values suggesting that the PM contained high amounts of heavy metals. Heavy metals interfere with the measurement of UV absorbance in cell viability tests. Compared with the LPS- and PM-treated groups, the levels of cyclo-oxygenase (COX)-2, phospho-p38 mitogen-activated protein kinase (MAPK), phospho-extracellular signal-regulated kinase 1/2, and phospho-c-Jun N-terminal kinase decreased significantly in the control group in a concentration-dependent manner (Fig. 2B and C). PM treatment also increased the levels of prostaglandin $E_2$ (PGE₂), interleukin (IL)-6, IL-1β, and tumor necrosis factor-α (TNF-α; Fig. 2D). FxRF treatment substantially attenuated PM-stimulated inflammatory responses and the expression levels of inflammatory mediators, including IL-1β, IL-6, PGE₂, and TNF-α, in HaCaT keratinocytes.

### 3.3. Protective activity of FxRF against PM-stimulated apoptotic body formation in keratinocytes

After conducting MTT assays to assess cell viability, DCFH-DA assays and Hoechst 33342 and PI staining were performed to further elucidate the protective effects of FxRF against PM-stimulated keratinocytes. Fluorescence microscopy images (Fig. 2E and F) showed significant apoptotic body formation in PM-exposed cells. However, apoptotic bodies were significantly downregulated in the FxRF-treated group in a concentration-dependent manner.

### 3.4. Protective effects of FxRF against PM-induced inflammatory responses in macrophages

As shown in Fig. 3A, NO production increased in PM- and LPS-stimulated macrophages. Moreover, the production of LPS-induced NO was higher than that of PM-induced NO. FxRF treatment decreased NO production but significantly increased the viability of PM-induced macrophages; this was observed for all concentrations. Key inflammatory regulators, such as iNOS and COX-2, indirectly regulated the levels of NO and PGE₂. PM stimulation significantly increased iNOS and COX-2 expression levels. However, FxRF treatment downregulated these targets in a concentration-dependent manner (Fig. 3B). Moreover, consistent with these observations, PM downregulated IL-1β and IL-6 compared with the effects of LPS (Fig. 3C). Additionally, compared with the control group, protein levels of TNF-α and PGE₂ were markedly decreased upon PM stimulation. These observations were consistent with those a previous study [24].
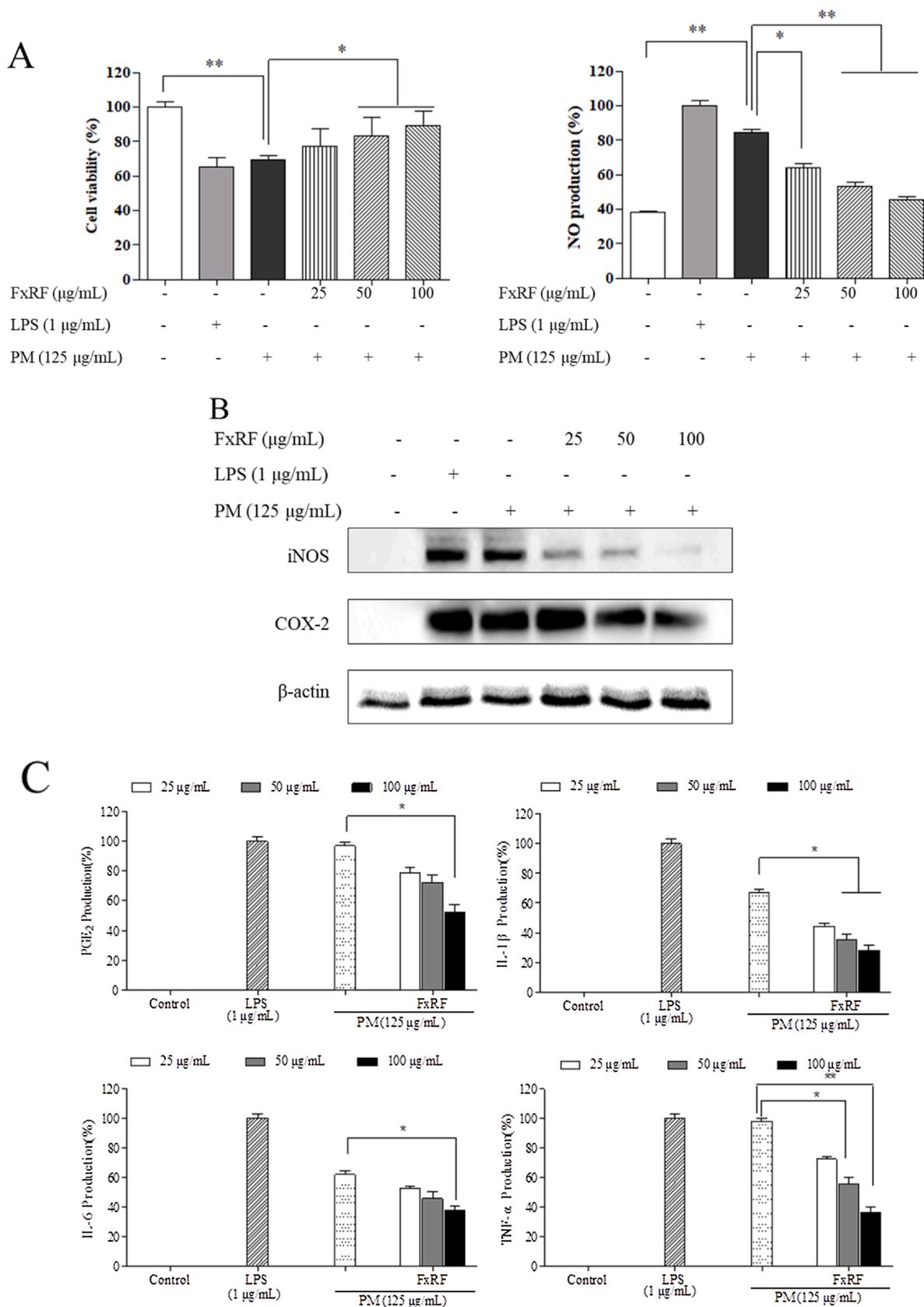
**Fig. 3.** Efficacy of FxRF against inflammation induced by PM in RAW 264.7 macrophages (A), and analyses of RAW cell viability and intracellular ROS levels; (B) Western blot analyses of iNOS and COX-2 expressions; and (C) ELISA of PGE$_2$ and pro-inflammatory cytokines (IL-1β, IL-6, and TNF-α). Pre-seeded cells (1 × 10$^5$ cells/mL) were treated with different FxRF concentrations after 24 h and stimulated with PM after 30 min. Cells were harvested after 24 h to measure inflammatory mediators (COX-2 and PGE$_2$) and pro-inflammatory cytokines (IL-1β, IL-6, and TNF-α). Graphical representations are means ± SE based on three replications. *$p <$ 0.05 and **$p <$ 0.01 indicate that the values were significantly different from those for the PM-treated group.
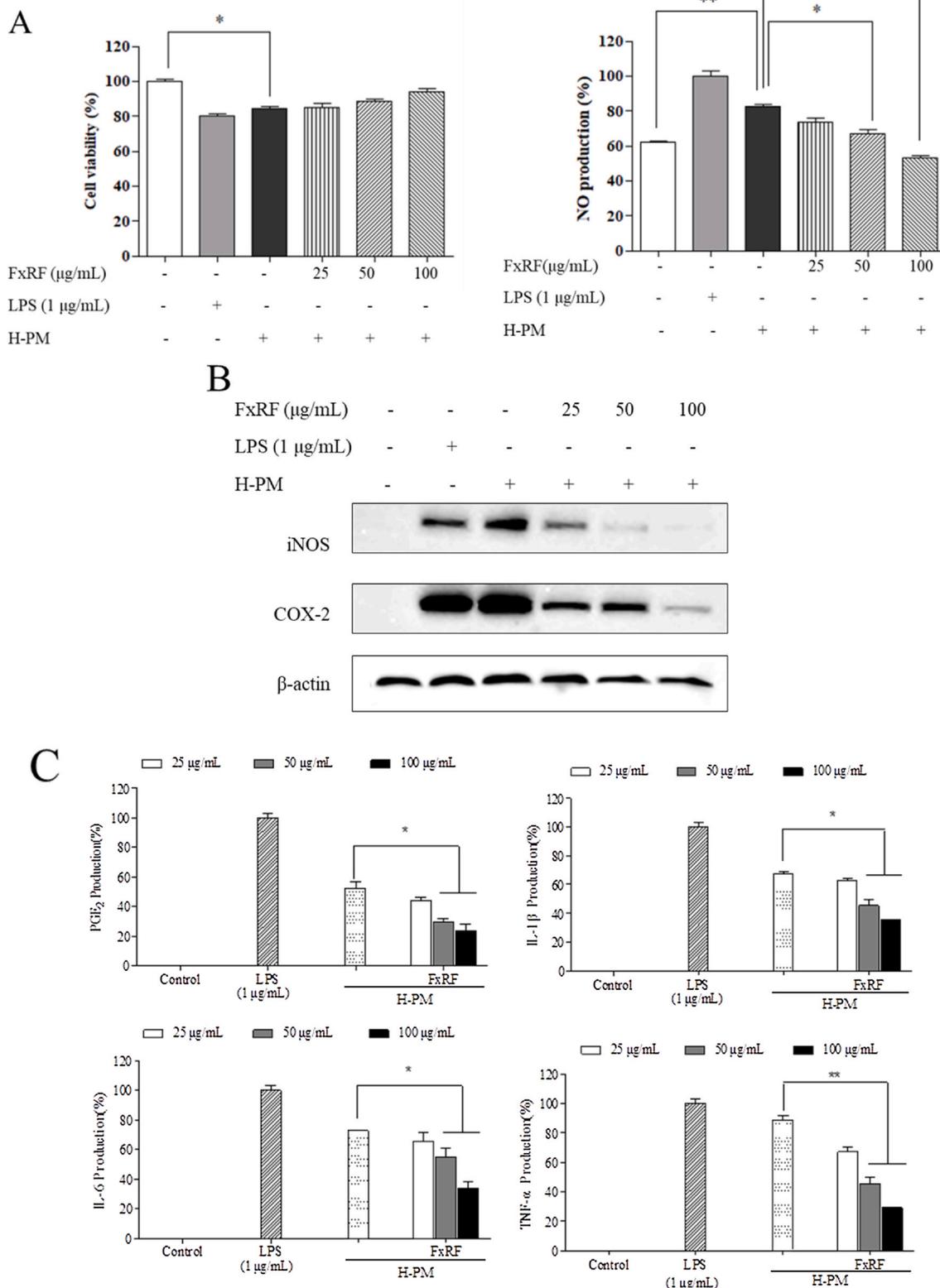
**Fig. 4.** Inflammatory stimulation of the RAW 264.7 macrophages by the culture medium of PM-induced HaCaT cells and the anti-inflammatory eff ;ects of FxRF: NO production and cytotoxicity (A), and analysis of iNOS and COX-2 levels (B) and inflammatory mediators (C), including tumor necrosis factor α (TNF-α), interleukin (IL)-1β, IL-6, and prostaglandin E2 (PGE$_2$). The HaCaT cells were pre-seeded in culture plates (1 × 10$^5$ cells/mL), incubated for 24 h, and treated with diff ;erent concentrations of FxRF. After 1 h, the cells were treated with PM (125 μg/mL) and 24 h later, the culture media were treated to each pre-seeded RAW 264.7 macrophages culture well plates in real time. The evaluations were made after a 24 h. Experiments were carried out in triplicate, and the results are represented as means ± SE. Values are significantly diff ;erent from the positive control (PM treated group) at *$p < 0.05$ and **$p < 0.001$. H-PM: The cultured medium of PM-stimulated in keratinocytes.
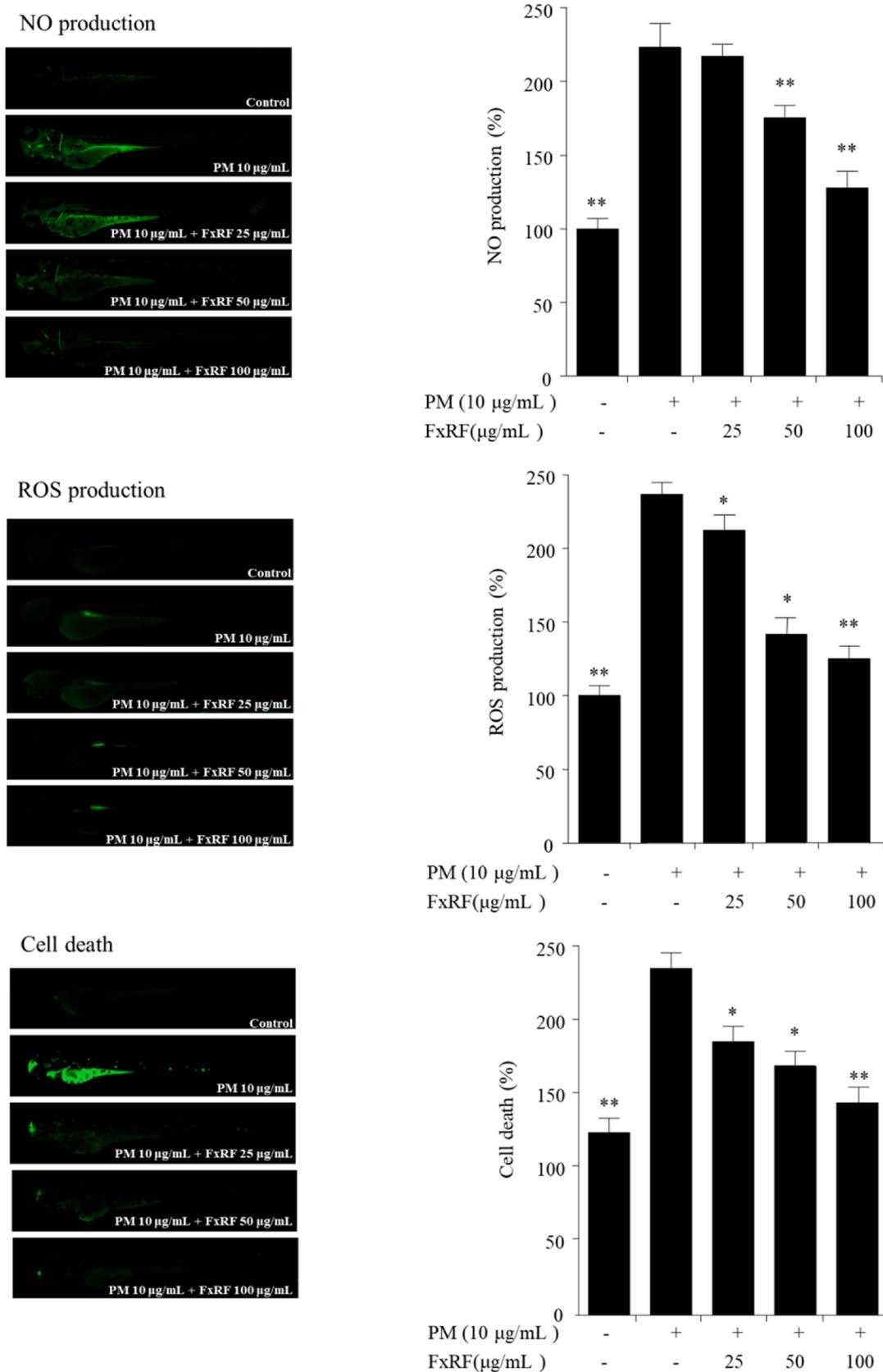
**Fig. 5.** Inflammatory stimulation of zebrafish larvae by PM and anti-inflammatory eff ;ects of FxRF: anti-inflammatory properties were evaluated by measuring NO and ROS production, and cell death in the zebrafish embryo model. Experiments were carried out in triplicate, and the results are represented as means $\pm$ SE. Values are significantly diff ;erent from the positive control (PM treated group) at *$p < 0.05$ and **$p < 0.001$.

## 3.5. Inflammatory responses in macrophages treated with the culture medium from PM-exposed FxRF-treated keratinocytes

Next, we evaluated the potential inflammatory responses in macrophages. Inflammatory responses were induced by medium from PM-stimulated keratinocytes. H-PM was transferred to macrophage culture plates, and inflammatory mediator levels were analyzed after 24 h of incubation. FxRF treatment markedly inhibited inflammatory responses in a concentration-dependent manner (Fig. 4A). Moreover, as the concentration of FxRF increased, iNOS and COX-2 levels were down-regulated (Fig. 4B). As depicted in Fig. 4C, compared with the control group, the H-PM group showed increased levels of all inflammatory mediators and cytokines in macrophages.

## 3.6. Anti-inflammatory effects of FxRF in a PM-exposed zebrafish embryo model

As shown in Fig. 5, low viability and high ROS and NO levels were observed in PM-exposed embryos compared with those in the control. However, the cell death rate of embryos decreased by 90 % following treatment with FxRF prior to PM treatment. FxRF treatment significantly decreased ROS and NO production in larvae, thereby protecting against PM-induced cell death. Interestingly, upon cell death, the cerebrum of PM-treated larvae exhibited a visible fluorescence intensity spot, indicating that PM may have the ability to damage the head tissue of larvae. Additionally, treatment of the embryos with FxRF strongly inhibited the inflammatory responses of PM in a concentration-dependent manner in zebrafish embryos. These results indicated that FxRF markedly decreased inflammatory responses in PM-exposed zebrafish embryos.

## 4. Discussion

PM is a serious public health concern in many developing countries. PM of less than 2.5 μm in size, known as PM 2.5, causes severe damage to the respiratory and circulatory systems [30]. Moreover, PM 2.5 also causes air pollution [31]. Notably, PM induces apoptosis in keratinocytes, which form the outer layer of the skin [32]. This induction of apoptosis leads to the production of secondary immune mediators, such as IL-1β and IL-6, by the surviving keratinocytes, resulting in the initiation of an inflammatory response [33]. The evidence of signal protein, such as p53 and TAp63, developing vertebrate keratinocyte and epidermis in breeding tubercles of the zebrafish was found [34]. The proinflammatory cytokines Il-1β and Tnf-α were controlled by macrophages in zebrafish [35]. Moreover, macrophages from zebrafish promote the healing of injury such as wounds [36]. Previous studies have indicated that the anti-inflammatory activity of diphlorethohydroxycarmalol against PM-stimulated responses in skin and immune cells [24]. Alginic acid from *S. horneri* has been shown to be useful against PM-induced inflammation in keratinocytes, RAW 264.7 macrophages, and zebrafish model [37]. Therefore, PM induces keratinocytes and transfers the inflammatory response to macrophages, and then PM stimulating apoptosis in zebrafish is promising.

Carotenoids are major pigments in seaweeds and have strong bio-activities [38,39]. In this study, FxRF was found to contain a mixture of five pigments, namely Fx, chlorophyll-a, β-carotene, cis-fucoxanthin, and pheophytin-a. These pigments have also been reported in other brown seaweeds [40]. Previous reports have observed the antioxidant ability of β-carotene [41] and the anti-inflammatory effects of chlorophyll-a [42]. Moreover, Fx reduces the levels of NO, PGE$_2$, IL-1β, TNF-α, and IL-6 *via* inhibition of the MAPK pathway in macrophages [43]. Hence, FxRF may be a promising active fraction for protection against PM-stimulated damage in macrophages, and the anti-inflammatory effects of FxRF are thought to be related to the presence of these five pigments. PM treatment decreased the viability of macrophages by 60%, whereas FxRF treatment resulted in cytoprotective activity against PM-stimulated inflammatory responses.

The MAPK signaling pathway is an extensively studied and well-known signaling pathway involved in various biological processes. Intracellular and extracellular materials related to inflammatory-associated cytokines and receptors mediate the MAPK pathway [43]. In our work, the inflammatory responses in PM-exposed keratinocytes were determined by measuring a series of cytokines and receptors, such as COX-2 and PGE$_2$. ROS production and cell viability were also measured. Comparison of LPS- and PM-induced inflammation revealed that the levels of cytokines and receptors decreased more in the latter group, and the decrease was dependent on PM concentration. This result highlighted the substantial anti-inflammatory effects of FxRF against PM.

## 5. Conclusion

In this study, we demonstrated that FxRF from *S. fusiformis* extracts exerted strong anti-inflammatory effects by attenuating PM-induced inflammation in macrophages and oxidative stress in keratinocytes. Collectively, our findings suggested that *S. fusiformis* may be a promising anti-inflammatory agent and an appropriate functional food ingredient.

## CRediT authorship contribution statement

**Yu-Lin Dai:** Methodology, Software, Validation. **Yun-Fei Jiang:** Visualization. **Yu-An Lu:** Validation, Data curation, Writing - original draft, Writing - review & editing. **Jiang-Bo Yu:** Validation, Formal analysis. **Min-Cheol Kang:** Conceptualization, Investigation, Resources, Project administration, Funding acquisition. **You-Jin Jeon:** Conceptualization, Supervision, Funding acquisition.

## Declaration of Competing Interest

The authors report no declarations of interest.

## Acknowledgements

## References

[1] V.V. Chernyshev, A.M. Zakharenko, S.M. Ugay, T.T. Hien, L.H. Hai, A.S. Kholodov, T.I. Burykina, A.K. Stratidakis, Y.O. Mezhuev, A.M. Tsatsakis, K.S. Golokhvast, Morphologic and chemical composition of particulate matter in motorcycle engine exhaust, Toxicol. Rep. 5 (2018) 224–230.

[2] V.V. Chernyshev, A.M. Zakharenko, S.M. Ugay, T.T. Hien, L.H. Hai, S.M. Olesik, A. S. Kholodov, E. Zubko, M. Kokkinakis, T.I. Burykina, A.K. Stratidakis, Y. O. Mezhuev, D.A. Sarigiannis, A. Tsatsakis, K.S. Golokhvast, Morphological and chemical composition of particulate matter in buses exhaust, Toxicol. Rep. 6 (2019) 120–125.

[3] C.K. Chan, X. Yao, Air pollution in mega cities in China, Atmos. Environ. 42 (2008) 1–42.

[4] K.S. Pikula, V.V. Chernyshev, A.M. Zakharenko, V.V. Chaika, G. Waissi, H. Le Hong, H. To Trong, A.M. Tsatsakis, K.S. Golokhvast, Toxicity assessment of particulate matter emitted from different types of vehicles on marine microalgae, Environ. Res. (2019) 179.

[5] S. Charlesworth, E. De Miguel, A. Ordóñez, A review of the distribution of particulate trace elements in urban terrestrial environments and its application to considerations of risk, Environ. Geochem. Health 33 (2011) 103–123.

[6] X. Hu, Y. Zhang, Z. Ding, T. Wang, H. Lian, Y. Sun, J. Wu, Bioaccessibility and health risk of arsenic and heavy metals (Cd, Co, Cr, Cu, Ni, Pb, Zn and Mn) in TSP and PM2. 5 in Nanjing, China, Atmos. Environ. 57 (2012) 146–152.

[7] J. Zhang, K.R. Smith, Household air pollution from coal and biomass fuels in China: measurements, health impacts, and interventions, Environ. Health Perspect. 115 (2007) 848–855.

[8] M. Diociaiuti, M. Balduzzi, B. De Berardis, G. Cattani, G. Stacchini, G. Ziemacki, A. Marconi, L. Paoletti, The two PM2. 5 (fine) and PM2. 5–10 (coarse) fractions: evidence of different biological activity, Environ. Res. 86 (2001) 254–262.

[9] R. Pozzi, B. De Berardis, L. Paoletti, C. Guastadisegni, Inflammatory mediators induced by coarse (PM2. 5–10) and fine (PM2. 5) urban air particles in RAW 264.7 cells, Toxicology 183 (2003) 243–254.

[10] Q. Li, Z. Kang, S. Jiang, J. Zhao, S. Yan, F. Xu, J. Xu, Effects of ambient fine particles PM2. 5 on human HaCaT cells, Int. J. Environ. Res. Public Health 14 (2017) 72.

[11] H. Choi, D.W. Shin, W. Kim, S.-J. Doh, S.H. Lee, M. Noh, Asian dust storm particles induce a broad toxicological transcriptional program in human epidermal keratinocytes, Toxicol. Lett. 200 (2011) 92–99.

[12] A. Fung, N. Hamid, J. Lu, Fucoxanthin content and antioxidant properties of Undaria pinnatifida, Food Chem. 136 (2013) 1055–1062.

[13] S.-J. Heo, Y.-J. Jeon, Protective effect of fucoxanthin isolated from Sargassum siliquastrum on UV-B induced cell damage, J. Photochem. Photobiol. B, Biol. 95 (2009) 101–107.

[14] K. Kanazawa, Y. Ozaki, T. Hashimoto, S.K. Das, S. Matsushita, M. Hirano, T. Okada, A. Komoto, N. Mori, M. Nakatsuka, Commercial-scale preparation of biofunctional fucoxanthin from waste parts of brown sea algae Laminalia japonica, Food Sci. Technol. Res. 14 (2008), 573-573.

[15] S.-J. Heo, S.-C. Ko, S.-M. Kang, H.-S. Kang, J.-P. Kim, S.-H. Kim, K.-W. Lee, M.-G. Cho, Y.-J. Jeon, Cytoprotective effect of fucoxanthin isolated from brown algae Sargassum siliquastrum against H 2 O 2-induced cell damage, Eur. Food Res. Technol. 228 (2008) 145–151.

[16] S.-J. Heo, W.-J. Yoon, K.-N. Kim, G.-N. Ahn, S.-M. Kang, D.-H. Kang, C. Oh, W.-K. Jung, Y.-J. Jeon, Evaluation of anti-inflammatory effect of fucoxanthin isolated from brown algae in lipopolysaccharide-stimulated RAW 264.7 macrophages, Food Chem. Toxicol. 48 (2010) 2045–2051.

[17] K.-N. Kim, S.-J. Heo, S.-M. Kang, G. Ahn, Y.-J. Jeon, Fucoxanthin induces apoptosis in human leukemia HL-60 cells through a ROS-mediated Bcl-xL pathway, Toxicol. Vitr. 24 (2010) 1648–1654.

[18] S.M. Kim, Y.-J. Jung, O.-N. Kwon, K.H. Cha, B.-H. Um, D. Chung, C.-H. Pan, A potential commercial source of fucoxanthin extracted from the microalga Phaeodactylum tricornutum, Appl. Biochem. Biotechnol. 166 (2012) 1843–1855.

[19] Y.-L. Dai, Y.-F. Jiang, H.G. Lee, Y.-J. Jeon, M.-C. Kang, Characterization and screening of anti-tumor activity of fucoidan from acid-processed hijiki (Hizikia fusiforme), Int. J. Biol. Macromol. 139 (2019) 170–180.

[20] Y.-L. Dai, Y.-F. Jiang, Y.-A. Lu, M.-c. Kang, Y.-J. Jeon, Fucoidan from acid-processed Hizikia fusiforme attenuates oxidative damage and regulate apoptosis, Int. J. Biol. Macromol. (2020).

[21] X. Yan, Y. Chuda, M. Suzuki, T. Nagata, Fucoxanthin as the major antioxidant in Hijikia fusiformis, a common edible seaweed, Biosci. Biotechnol. Biochem. 63 (1999) 605–607.

[22] Y.-L. Dai, M.-D. Qiao, P. Yu, F. Zheng, H. Yue, S.-Y. Liu, Comparing eight types of ginsenosides in ginseng of different plant ages and regions using RRLC-Q-TOF MS/MS, J. Ginseng Res. 44 (2020) 205–214.

[23] L.-J. Wang, Y. Fan, R. Parsons, G.-R. Hu, P.-Y. Zhang, F.-L. Li, A rapid method for the determination of fucoxanthin in diatom, Mar. Drugs 16 (2018) 33.

[24] I. Fernando, H.-S. Kim, K. Sanjeewa, J.-Y. Oh, Y.-J. Jeon, W.W. Lee, Inhibition of inflammatory responses elicited by urban fine dust particles in keratinocytes and macrophages by diphlorethohydroxycarmalol isolated from a brown alga Ishige okamurae, Algae 32 (2017) 261–273.

[25] Y.-L. Dai, E.-A. Kim, H.-M. Luo, Y.-F. Jiang, J.-Y. Oh, S.-J. Heo, Y.-J. Jeon, Characterization and anti-tumor activity of saponin-rich fractions of South Korean sea cucumbers (Apostichopus japonicus), J. Food Sci. Technol. (2020) 1–10.

[26] E.-A. Kim, S.-H. Lee, C.-i. Ko, S.-H. Cha, M.-C. Kang, S.-M. Kang, S.-C. Ko, W.-W. Lee, J.-Y. Ko, J.-H. Lee, Protective effect of fucoidan against AAPH-induced oxidative stress in zebrafish model, Carbohydr. Polym. 102 (2014) 185–191.

[27] Y.-L. Dai, Y.-F. Jiang, Y.-H. Nie, Y.-A. Lu, M.-K. Kang, Y.-J. Jeon, Hepato-protective effect of fucoidan extracted from acid-processed Sargassum fusiformis in ethanol-treated Chang liver cells and in a zebrafish model, J. Appl. Phycol. 32 (6) (2020) 4289–4298.

[28] T. Maoka, Y. Fujiwara, K. Hashimoto, N. Akimoto, Rapid Identification of carotenoids in a combination of liquid chromatography/UV-visible absorption spectrometry by photodiode-array detector and atmospheric pressure chemical ionization mass spectrometry (LC/PAD/APCI-MS), J. Oleo Sci. 51 (2002) 1–9.

[29] G. Rajauria, B. Foley, N. Abu-Ghannam, Characterization of dietary fucoxanthin from Himanthalia elongata brown seaweed, Food Res. Int. 99 (2017) 995–1001.

[30] X. Zeng, X. Xu, X. Zheng, T. Reponen, A. Chen, X. Huo, Heavy metals in PM2. 5 and in blood, and children's respiratory symptoms and asthma from an e-waste recycling area, Environ. Pollut. 210 (2016) 346–353.

[31] K. Pikula, V. Chaika, A. Zakharenko, A. Savelyeva, I. Kirsanova, A. Anisimova, K. Golokhvast, Toxicity of Carbon, Silicon, and Metal-Based Nanoparticles to the Hemocytes of Three Marine Bivalves, Animals (2020) 10.

[32] R. Hu, X.-Y. Xie, S.-K. Xu, Y.-N. Wang, M. Jiang, L.-R. Wen, W. Lai, L. Guan, PM2. 5 exposure elicits oxidative stress responses and mitochondrial apoptosis pathway activation in HaCaT keratinocytes, Chin. Med. J. 130 (2017) 2205.

[33] Y. Zhang, L. Zheng, J. Tuo, Q. Liu, X. Zhang, Z. Xu, S. Liu, G. Sui, Analysis of PM2. 5-induced cytotoxicity in human HaCaT cells based on a microfluidic system, Toxicol. Vitr. 43 (2017) 1–8.

[34] B. Fischer, M. Metzger, R. Richardson, P. Knyphausen, T. Ramezani, R. Franzen, E. Schmelzer, W. Bloch, T.J. Carney, M. Hammerschmidt, p53 and TAp63 promote keratinocyte proliferation and differentiation in breeding tubercles of the zebrafish, PLoS Genet. 10 (2014), e1004048.

[35] T.M. Tsarouchas, D. Wehner, L. Cavone, T. Munir, M. Keatinge, M. Lambertus, A. Underhill, T. Barrett, E. Kassapis, N. Ogryzko, Dynamic control of proinflammatory cytokines Il-1β and Tnf-α by macrophages in zebrafish spinal cord regeneration, Nat. Commun. 9 (2018) 1–17.

[36] Y.-Y. Liu, J.-Q. Wu, R.-Y. Fan, Z.-H. He, C.-Y. Li, M.-F. He, Isoliquiritin promote angiogenesis by recruiting macrophages to improve the healing of zebrafish wounds, Fish Shellfish Immunol. (2020).

[37] I.S. Fernando, T.U. Jayawardena, K.A. Sanjeewa, L. Wang, Y.-J. Jeon, W.W. Lee, Anti-inflammatory potential of alginic acid from Sargassum horneri against urban aerosol-induced inflammatory responses in keratinocytes and macrophages, Ecotoxicol. Environ. Saf. 160 (2018) 24–31.

[38] D. Giuffrida, F. Cacciola, P. Mapelli-Brahm, C.M. Stinco, P. Dugo, M. Oteri, L. Mondello, A.J. Meléndez-Martínez, Free carotenoids and carotenoids esters composition in Spanish orange and mandarin juices from diverse varieties, Food Chem. 300 (2019) 125139.

[39] K.-J. Yeum, R.M. Russell, Carotenoid bioavailability and bioconversion, Annu. Rev. Nutr. 22 (2002) 483–504.

[40] A.R.-B. de Quirós, S. Frecha-Ferreiro, A. Vidal-Perez, J. López-Hernández, Antioxidant compounds in edible brown seaweeds, Eur. Food Res. Technol. 231 (2010) 495–498.

[41] J. Terao, Antioxidant activity of β-carotene-related carotenoids in solution, Lipids 24 (1989) 659–661.

[42] A. Subramoniam, V.V. Asha, S.A. Nair, S.P. Sasidharan, P.K. Sureshkumar, K. N. Rajendran, D. Karunagaran, K. Ramalingam, Chlorophyll revisited: Anti-inflammatory activities of chlorophyll a and inhibition of expression of TNF-α gene by the same, Inflammation 35 (2012) 959–966.

[43] K.-N. Kim, S.-J. Heo, W.-J. Yoon, S.-M. Kang, G. Ahn, T.-H. Yi, Y.-J. Jeon, Fucoxanthin inhibits the inflammatory response by suppressing the activation of NF-κB and MAPKs in lipopolysaccharide-induced RAW 264.7 macrophages, Eur. J. Pharmacol. 649 (2010) 369–375.